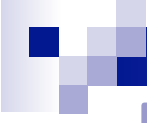




## Part 2

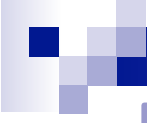
# **Submesoscale dynamics**



# Dynamics at the ocean submesoscales

Characteristic scales:

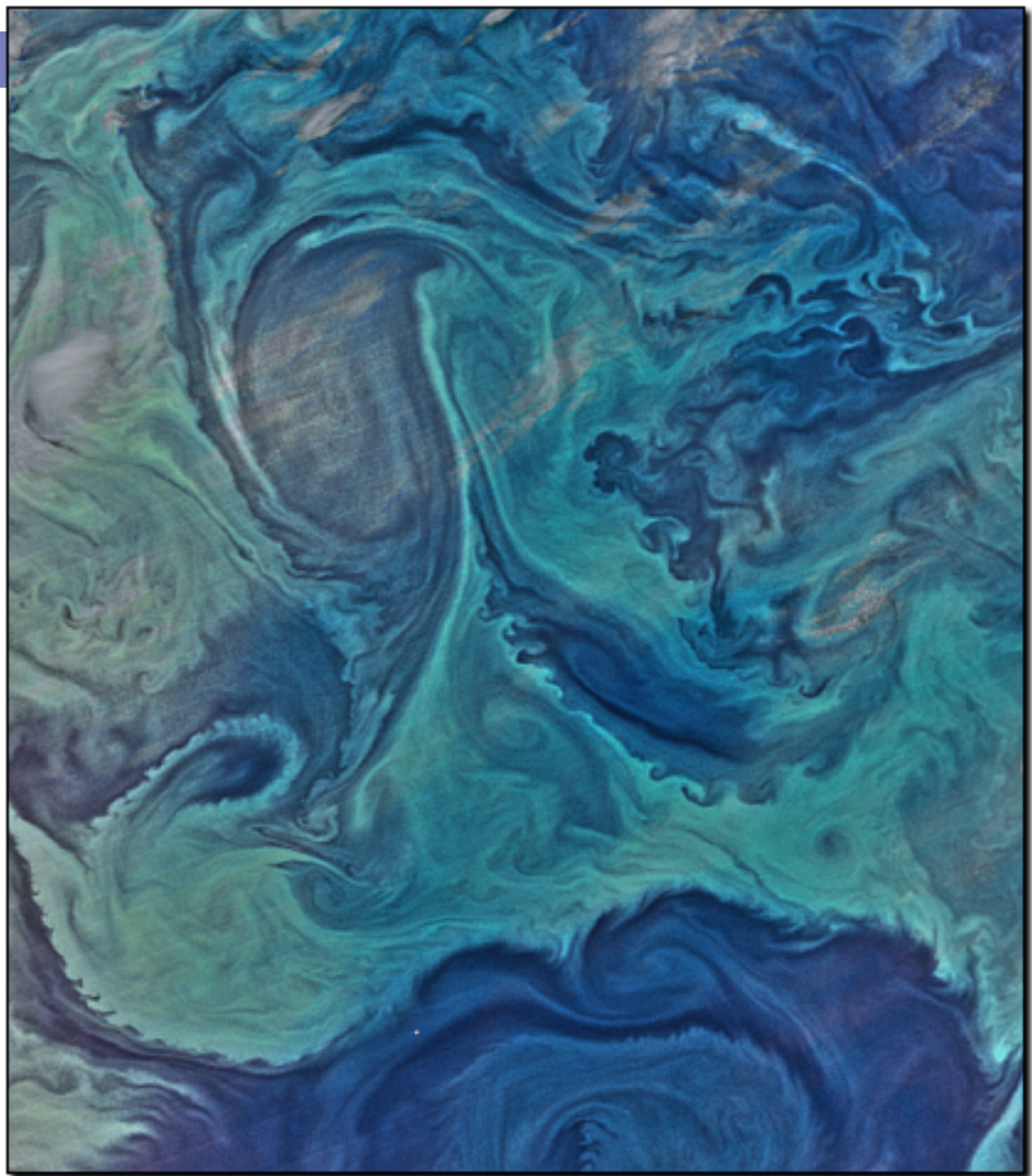
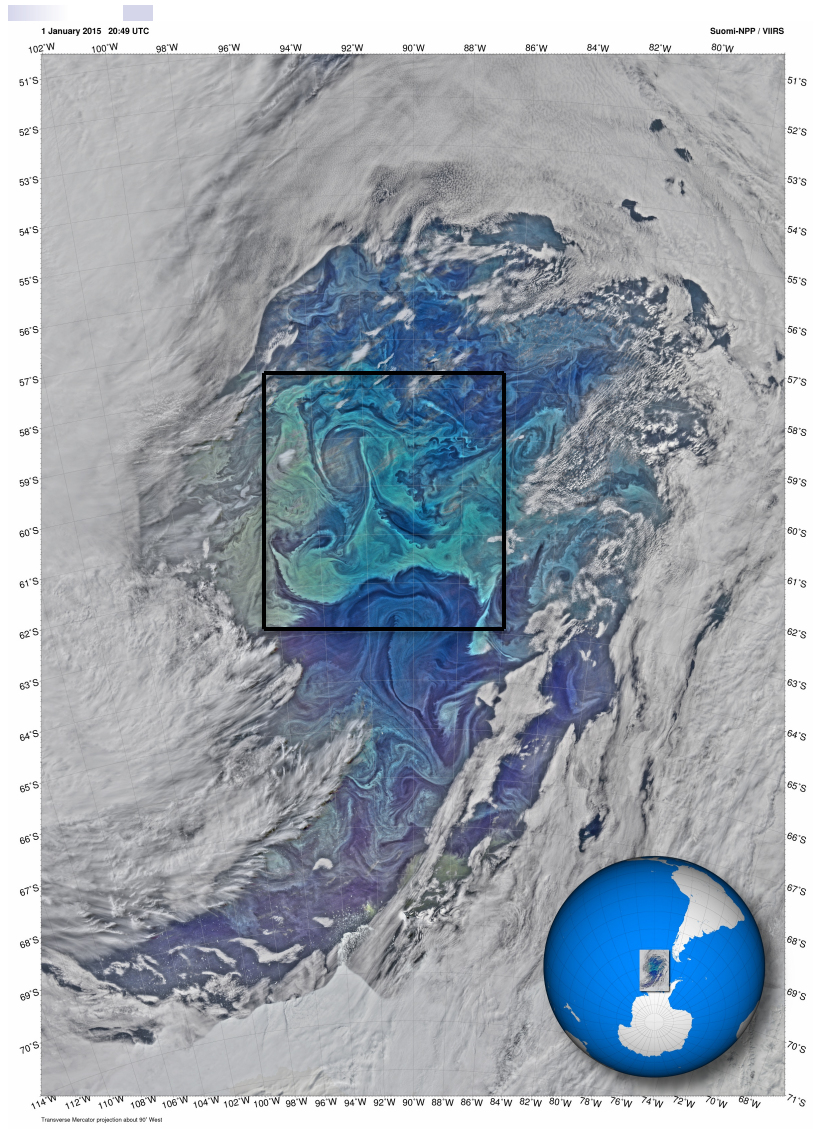
- $L \sim 100 \text{ m} - 10 \text{ km}$  (here  $\geq 1 \text{ km}$ )
  - $H \sim 10 - 100 \text{ m}$
  - $t \sim \text{hours} - \text{few weeks}$  (here  $\geq 1 \text{ day}$ )
- 
- ◆ Rotation and stratification are still important but are not asymptotically overwhelming
  - ◆ Ageostrophic motions cannot be neglected



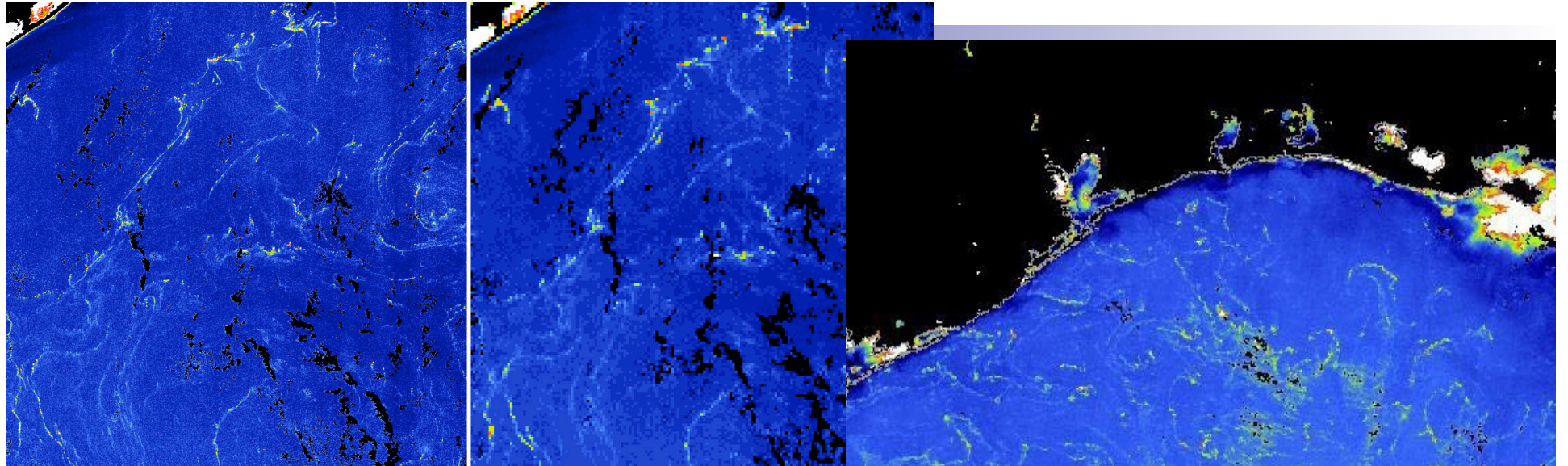
# Dynamics at the ocean submesoscales

- Arise from **mesoscale eddies** and boundary currents (or interactions with **bottom topography**) in the form of surface-layer fronts, vorticity filaments, small coherent vortices.
- Associated with large APE->EKE transfers through **mixed-layer instabilities and frontogenesis**
- Dynamics are mostly advective and only partly “balanced” with  $R_o = V/fL \sim 1$
- Strong surface convergences and vertical velocity, hence vertical fluxes

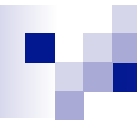
- Limited measurements
- Most progress in our understanding through modeling using nested techniques to investigate finer and finer scales
- Approaching the limits of hydrostatic models



**Observations: Phytoplankton bloom around Antarctica**  
January 15, 2015. Modis AQUA

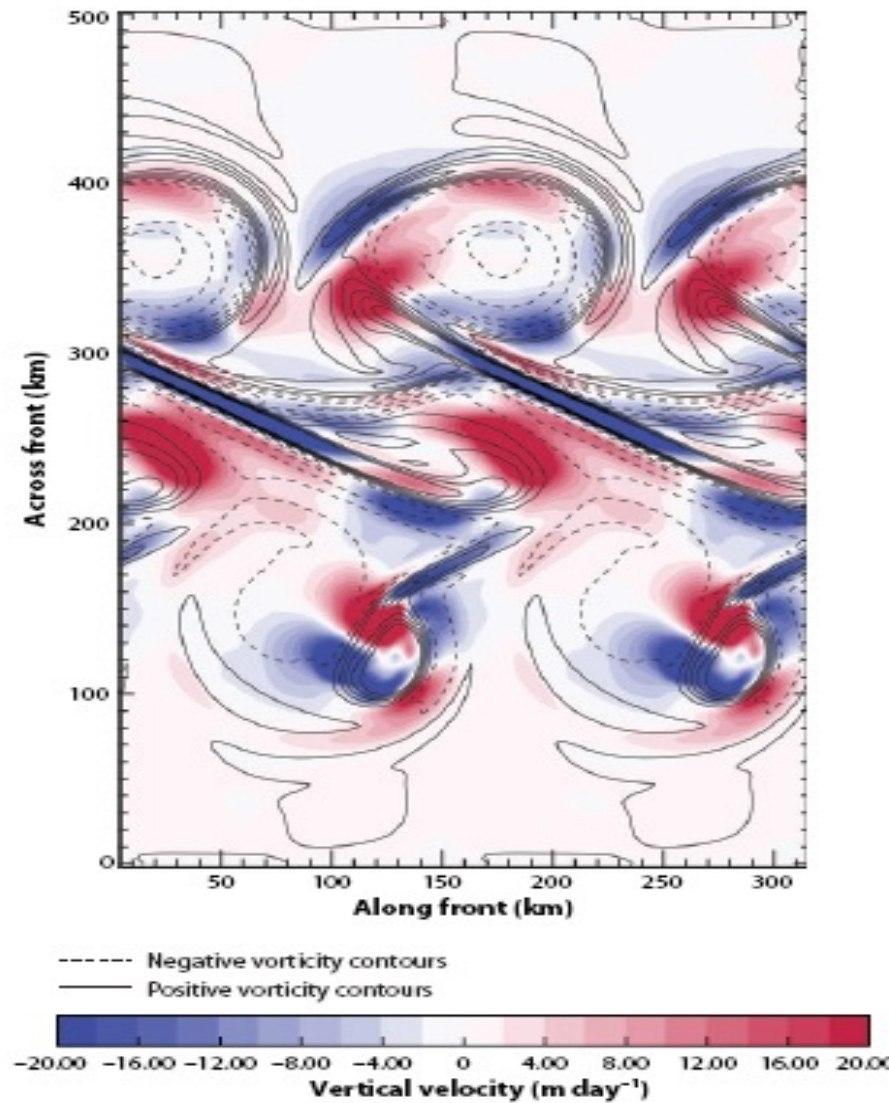


**Observations in the Gulf of Mexico**  
MERCI MCI (Max. Chl Intensity)  
images of Sargassum lines in  
2005  
(Gower et al., 2006)

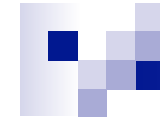


# Ageostrophic (unbalanced) motions cannot be neglected

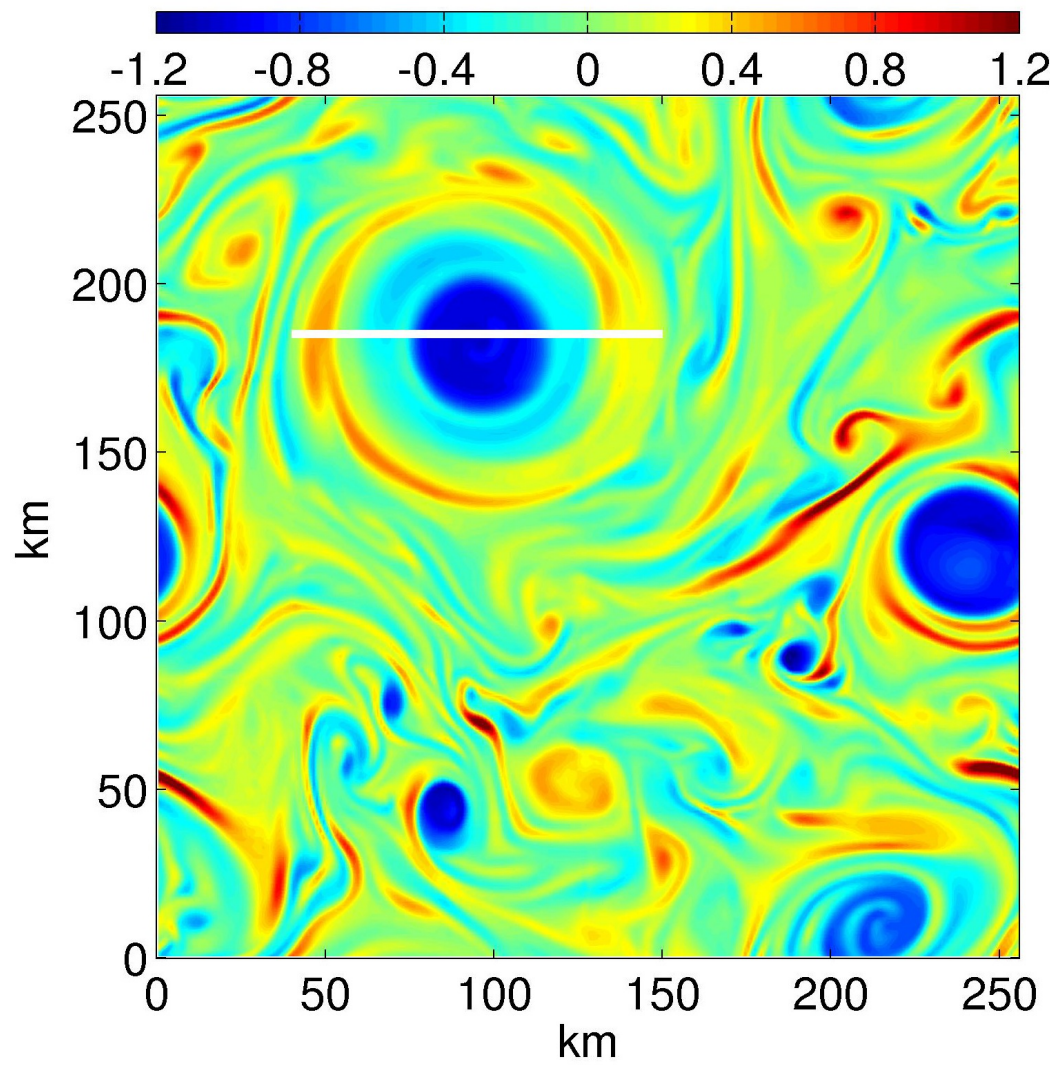
Klein and Lamyere,  
Ann. Rev. Marine  
Science, 2009



Vertical velocities  
at 90 m (*red for  
upward and blue  
for downward* )  
around a front.



# Vorticity Field, $\zeta/f$



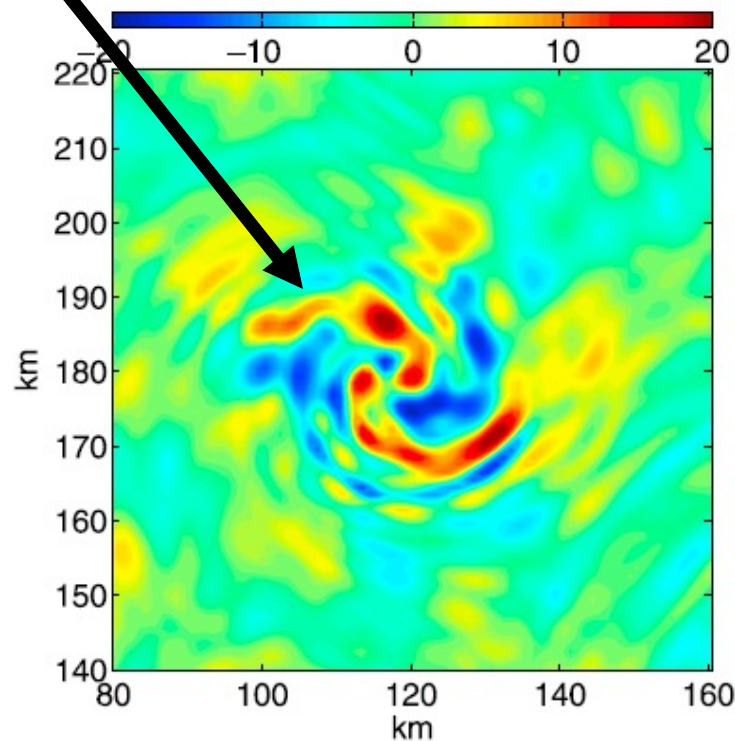
Koszalka  
et al, JGR  
2009

Looks even more complicated if we do not average over one day...

Vortex Rossby waves

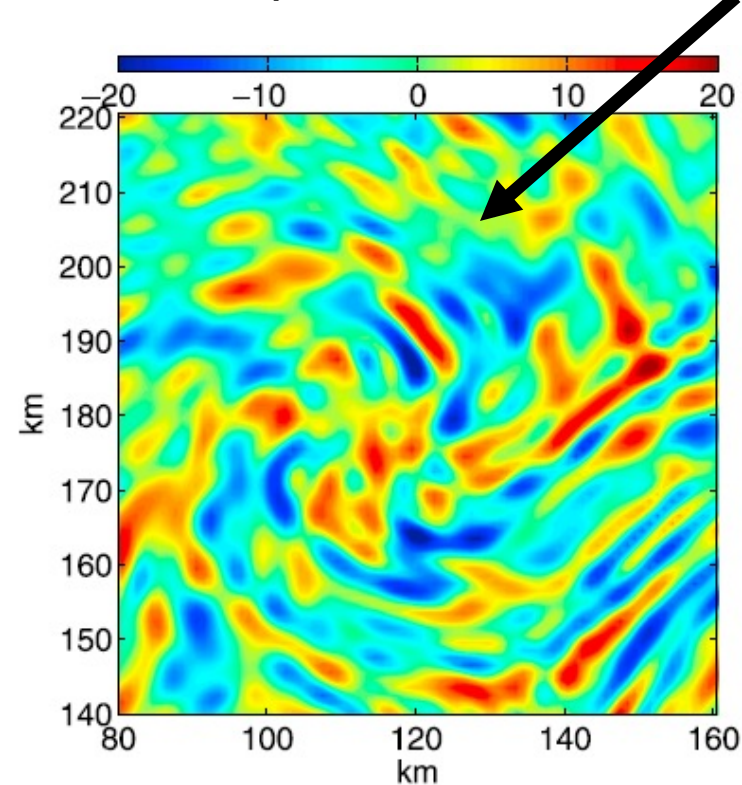
VRW

again 78 and 350m, in m/day



near-inertial oscillations

NIO



# VERTICAL TRANSPORT: Eddies and internal waves

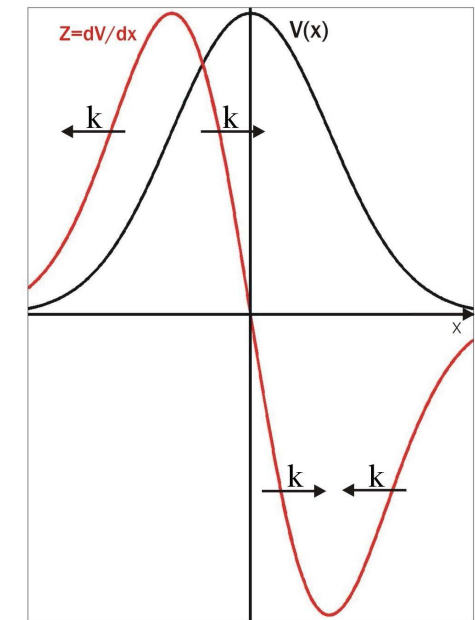
Kunze (1985) shows that eddies ‘polarize’ near inertial waves. Anticyclones trap them and reflect the energy downward, while cyclones expel them.

$$u(\vec{x}, t) \approx u_o \sin\left(ft + \frac{Z}{2}t\right) \approx u_o \sin\left(ft + \frac{Z_o}{2}t - \vec{k} \cdot \vec{x}\right)$$

Mechanism: Winds with energy in the f band excite inertial waves at the ocean surface. The frequency of the excited oceanic wave depends on f corrected by  $Z/2$  (near inertial).

Cyclones end up with  $f_{\text{eff}} > f$  and the waves can propagate outside. In anticyclones  $f_{\text{eff}} < f$  and NIW are trapped.

Refraction by relative vorticity causes a decrease in NIW scale accelerating their vertical propagation.

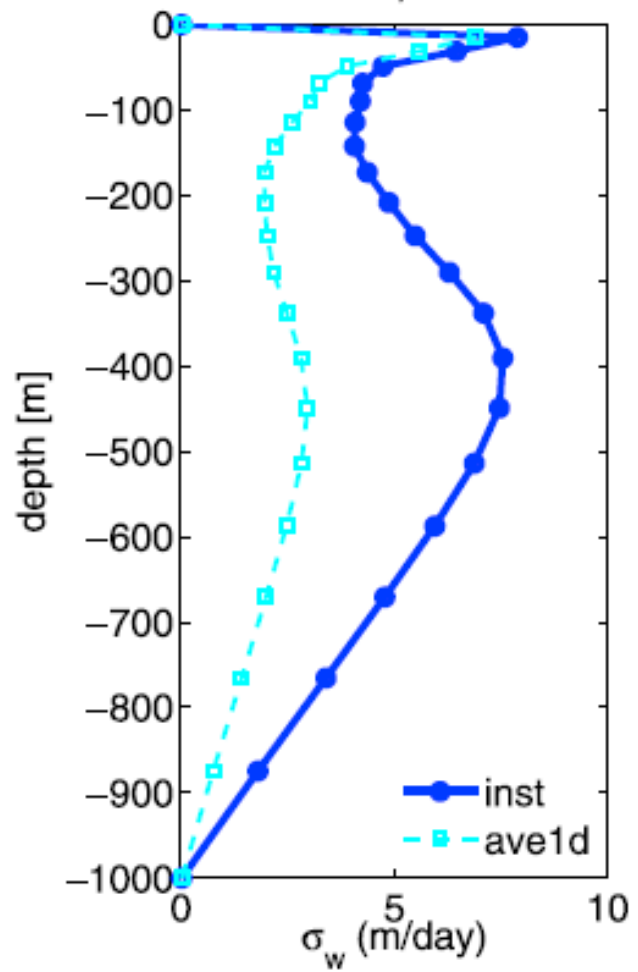


$$k = -\frac{\partial Z}{\partial x} \frac{t}{2}$$

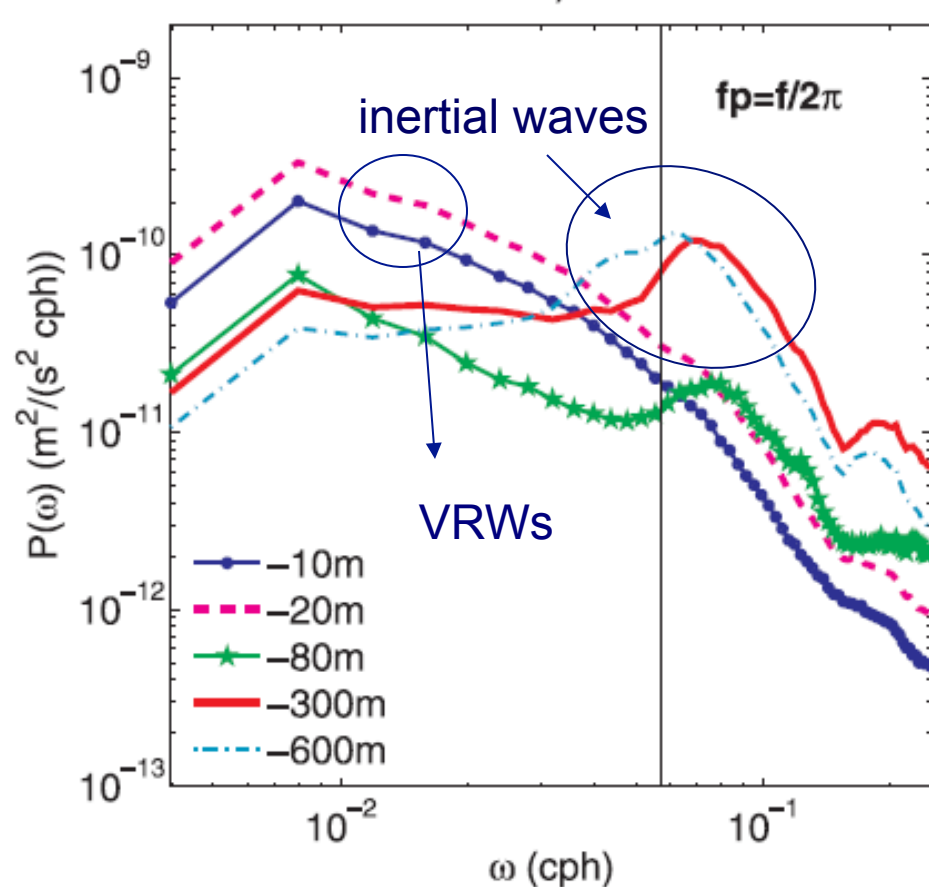
schematic by P. Klein

(Danioux and Klein, 2008; Danioux et al. 2008, 2011)

standard deviation  
vertical velocity field



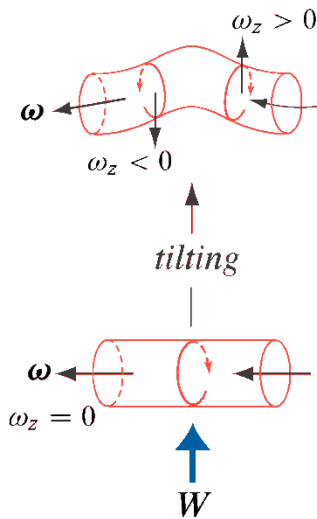
frequency spectra



# Diagnosing the vertical velocity field

$w = \text{FREE SURFACE} +$

$\text{ADVECTION (AGEOSTROPHIC)} +$

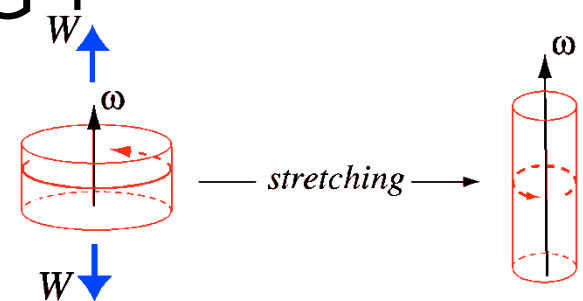


$\text{STRETCHING} + \text{TLTING} +$

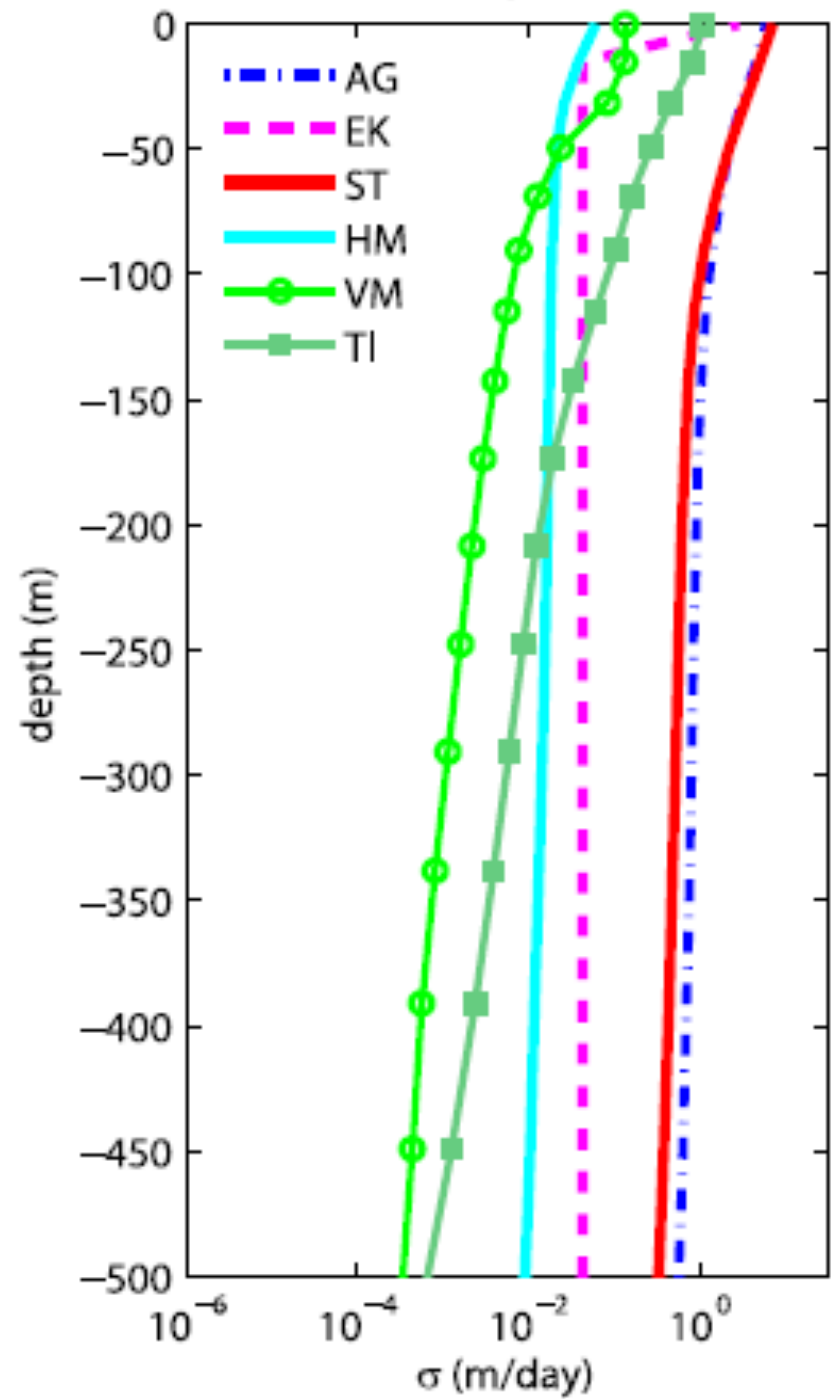
$\text{EKMAN} +$

$\text{HORIZONTAL MIXING} +$

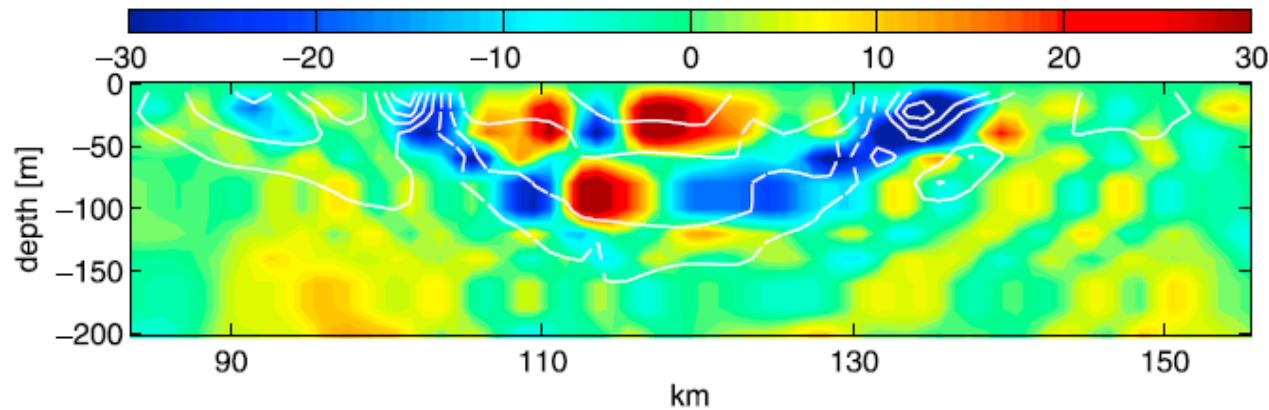
$\text{VERTICAL MIXING}$



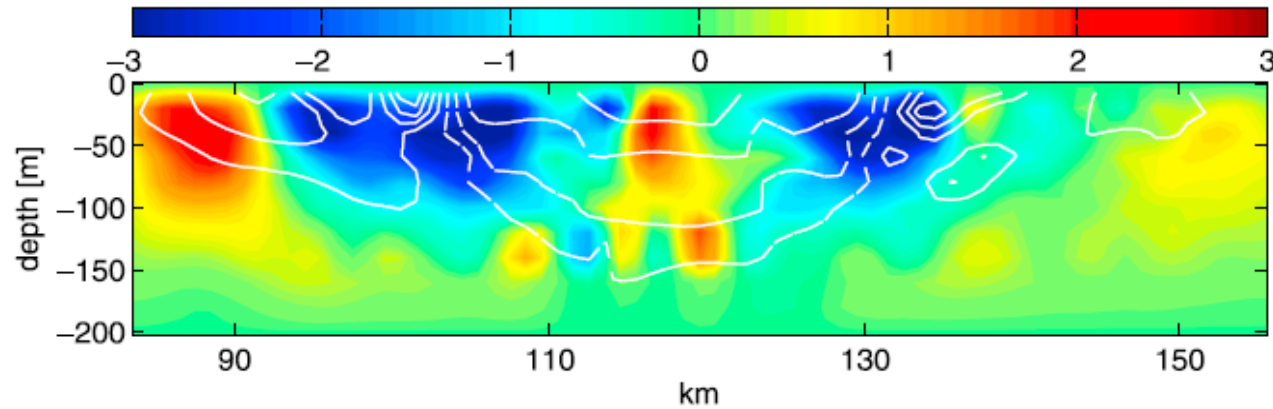
$$\begin{aligned}
& \text{FREE SURFACE} \\
w(x, y, z) = & \frac{D\eta}{Dt} \\
& - \int_z^\eta \alpha_1 \left[ \frac{\partial \zeta_1}{\partial t} + u \frac{\partial \zeta_1}{\partial x} + v \frac{\partial \zeta_1}{\partial y} + w \frac{\partial \zeta_1}{\partial z} \right] dz \\
& - \int_z^\eta \alpha_2 \left[ \frac{\partial \zeta_2}{\partial t} + u \frac{\partial \zeta_2}{\partial x} + v \frac{\partial \zeta_2}{\partial y} + w \frac{\partial \zeta_2}{\partial z} \right] dz \\
& - \int_z^\eta \alpha_1 [\chi_2 \zeta_1] dz - \int_z^\eta \alpha_2 [\chi_1 \zeta_2] dz \\
& - \int_z^\eta \alpha_1 \left[ \frac{\partial w}{\partial x} \frac{\partial v}{\partial z} \right] dz + \int_z^\eta \alpha_2 \left[ \frac{\partial w}{\partial y} \frac{\partial u}{\partial z} \right] dz \\
& + \int_z^\eta \frac{\alpha_2}{\rho_o} \left[ - \frac{\partial}{\partial y} \frac{\partial \tau_x}{\partial z} \right] dz \\
& + \sum_{i=1,2} \int_z^\eta \alpha_i A_H \left( \frac{\partial^4 \zeta_i}{\partial x^4} + \frac{\partial^4 \zeta_i}{\partial y^4} \right) dz \\
& + \int_z^\eta \alpha_1 \frac{\partial}{\partial x} \frac{\partial}{\partial z} \left( K_v \frac{\partial v}{\partial z} \right) dz - \int_z^\eta \alpha_2 \frac{\partial}{\partial y} \frac{\partial}{\partial z} \left( K_v \frac{\partial u}{\partial z} \right) dz \\
& \zeta_1 = \frac{\partial v}{\partial x}; \quad \zeta_2 = - \frac{\partial u}{\partial y}; \quad \chi_1 = \frac{\partial u}{\partial x}; \quad \chi_2 = \frac{\partial v}{\partial y} \\
& \alpha_1 = (f + \zeta_1)^{-1}; \quad \alpha_2 = (f + \zeta_2)^{-1}
\end{aligned}$$

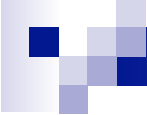


with primitive equations (ROMS)

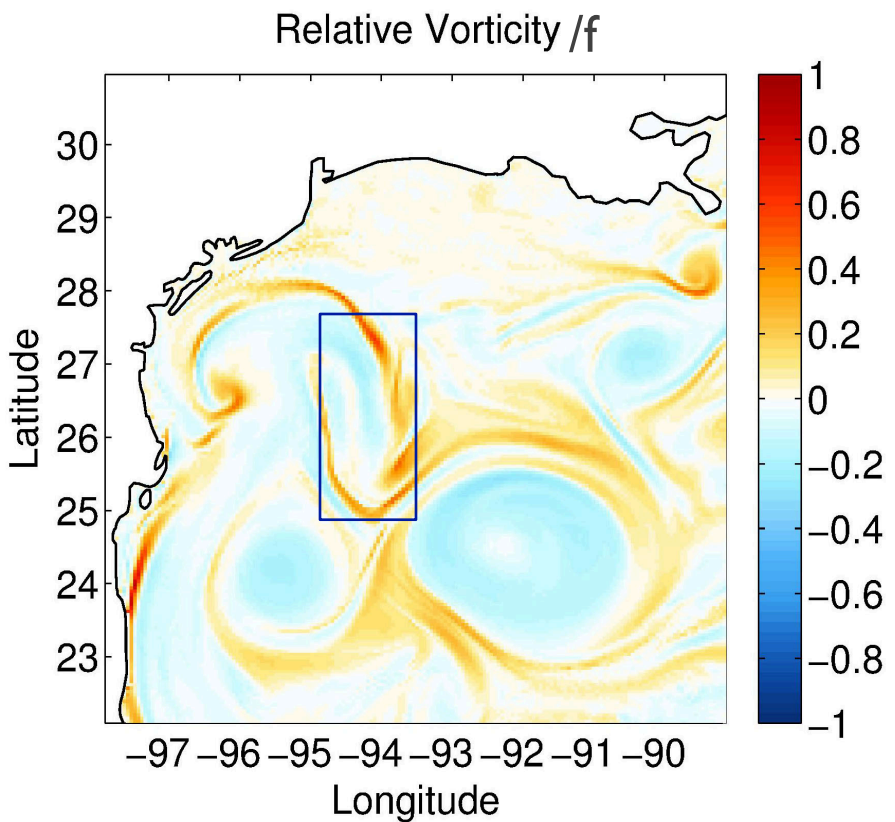
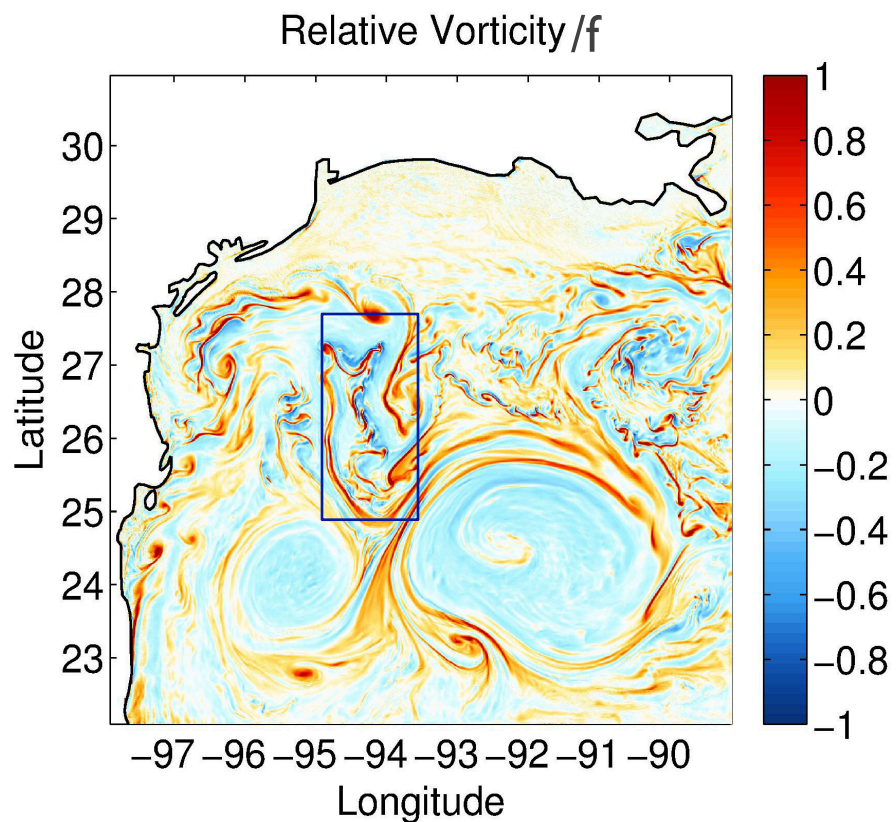


with the omega-equation



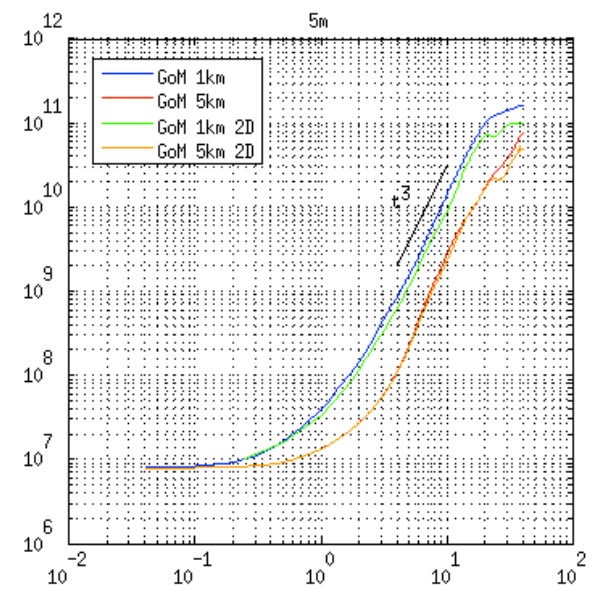
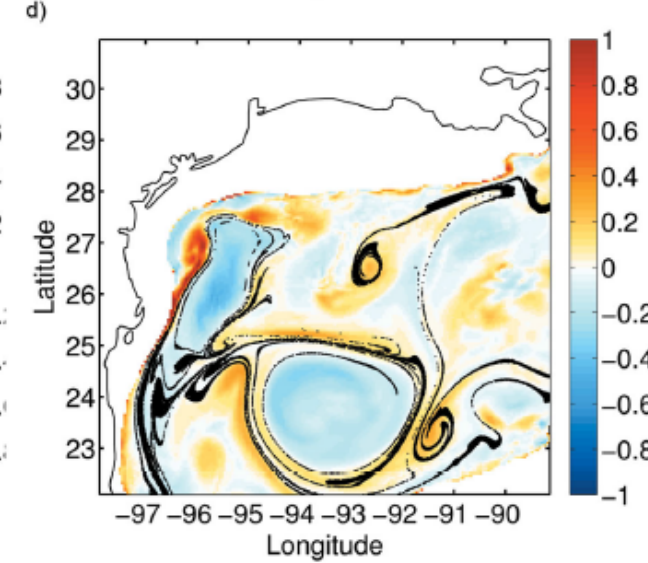
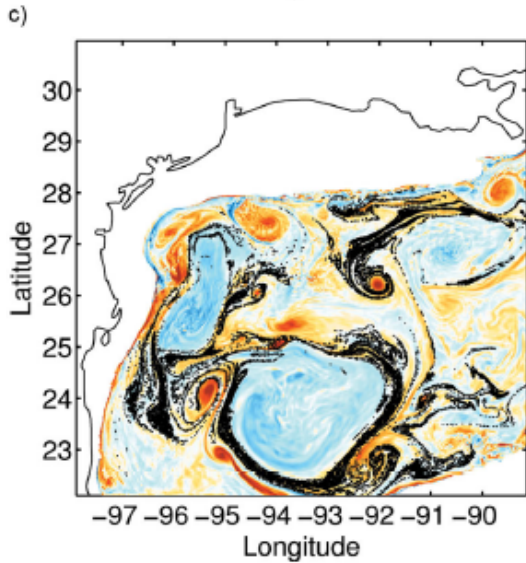
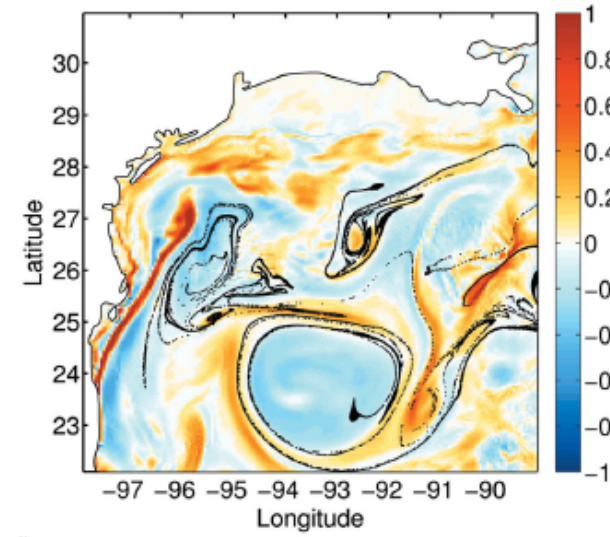
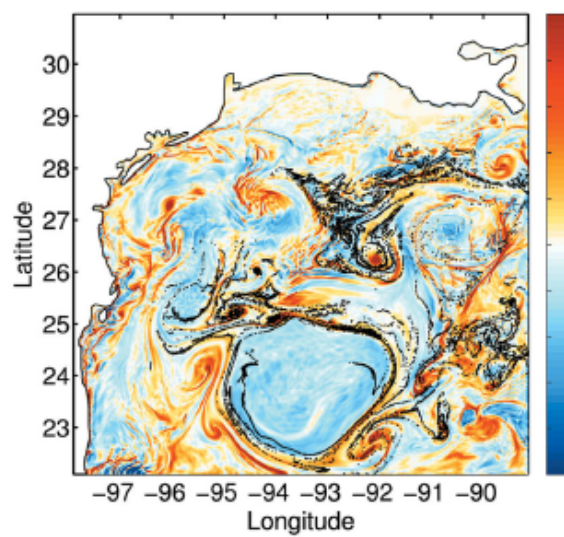


## And in a realistic set-up (Gulf of Mexico)



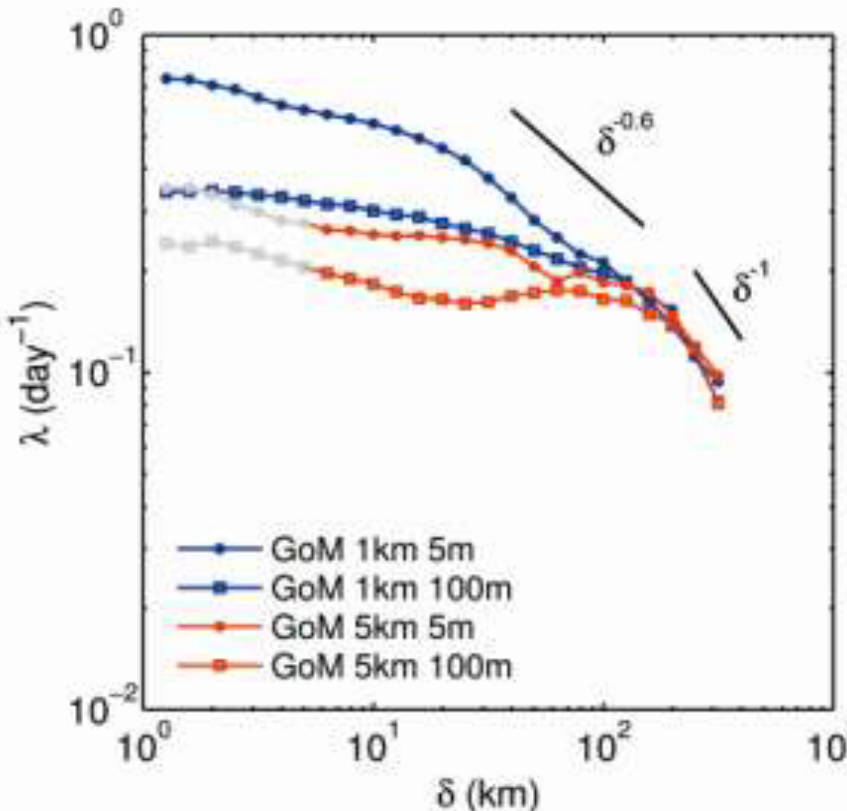
Zhong and Bracco, 2013

# HORIZONTAL TRANSPORT: Relative dispersion

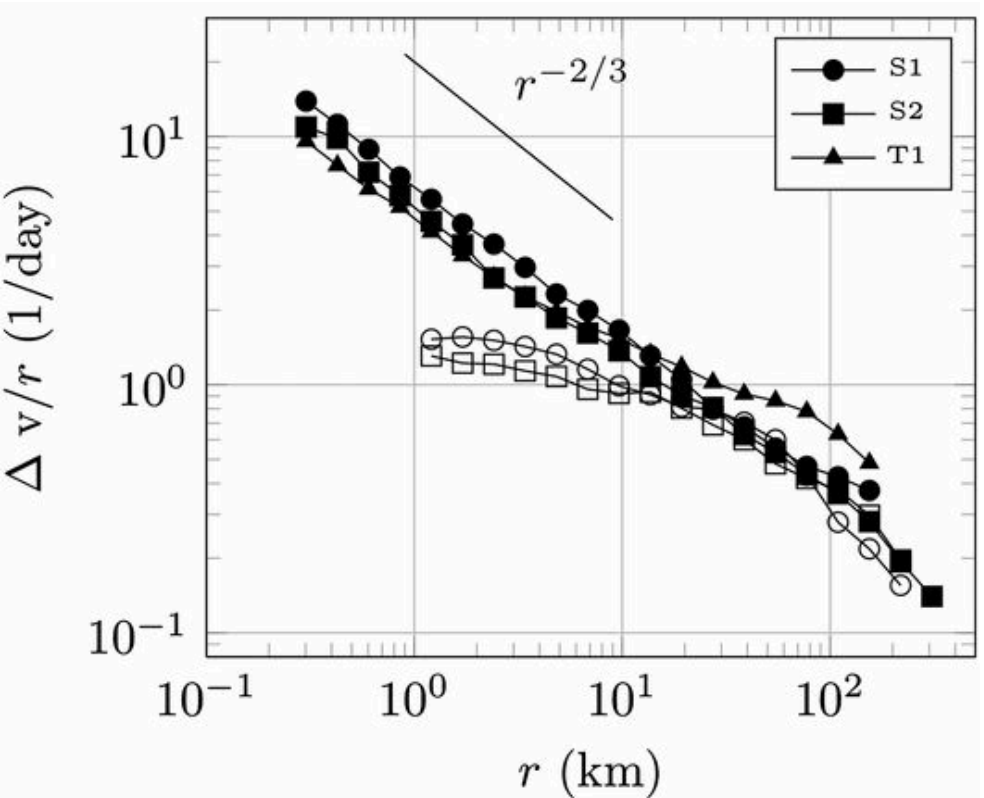


Relative dispersion for  
2d and 3d particles  
deployed at 5m depth

# FSLE: scale-dependent pair separation rate as function of separation distance

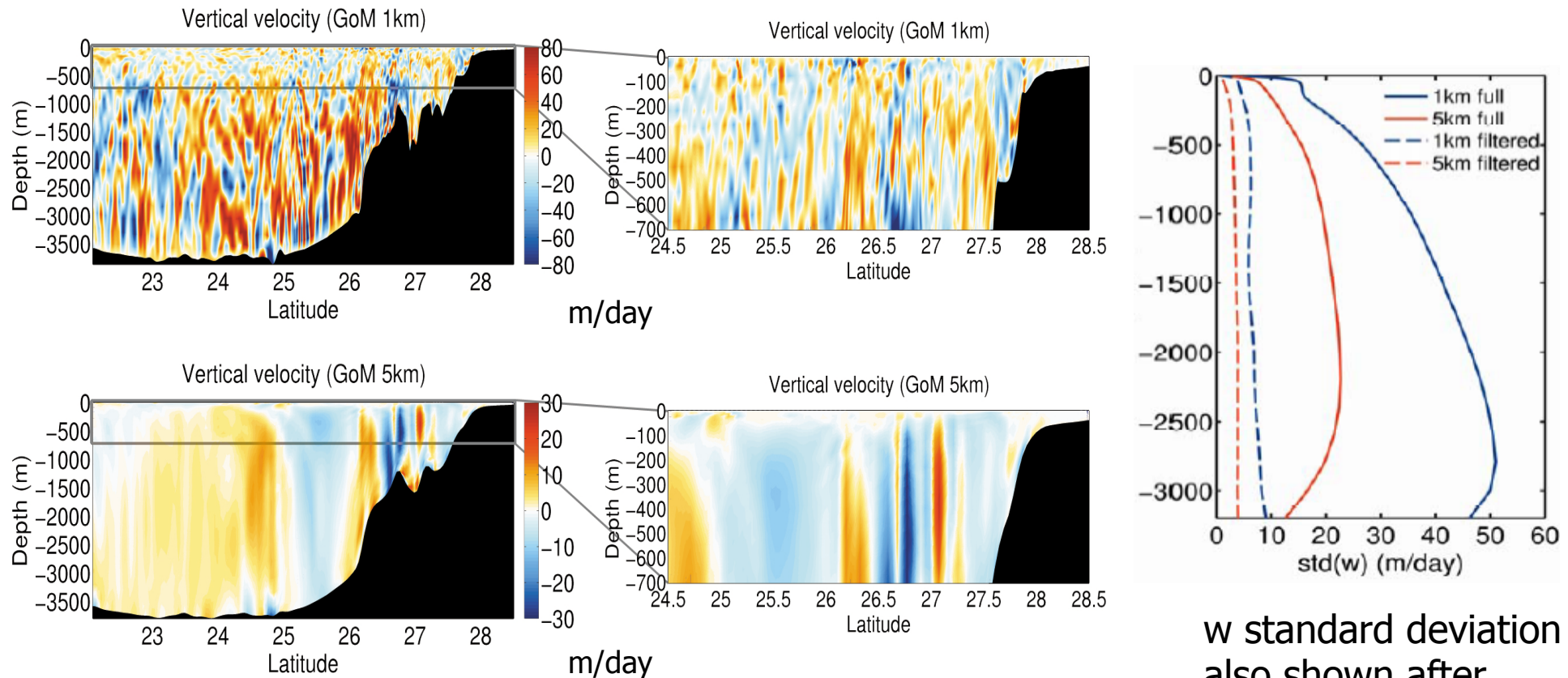


ROMS



GLAD observations, Northern Gulf,  
summer 2012 and NCOM 3km  
model (Poje et al., PNAS 2014)

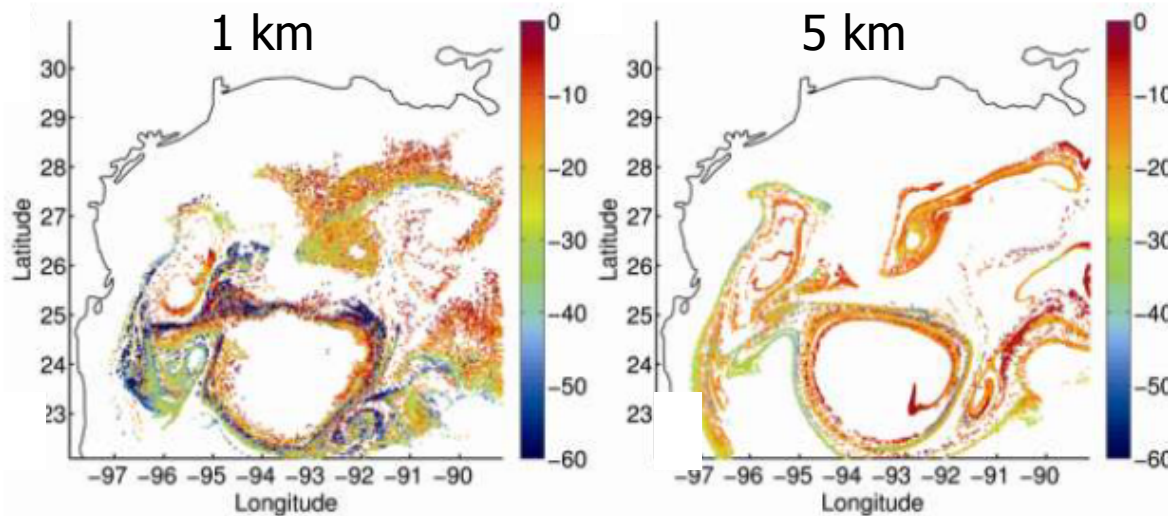
# VERTICAL TRANSPORT: Vertical velocities



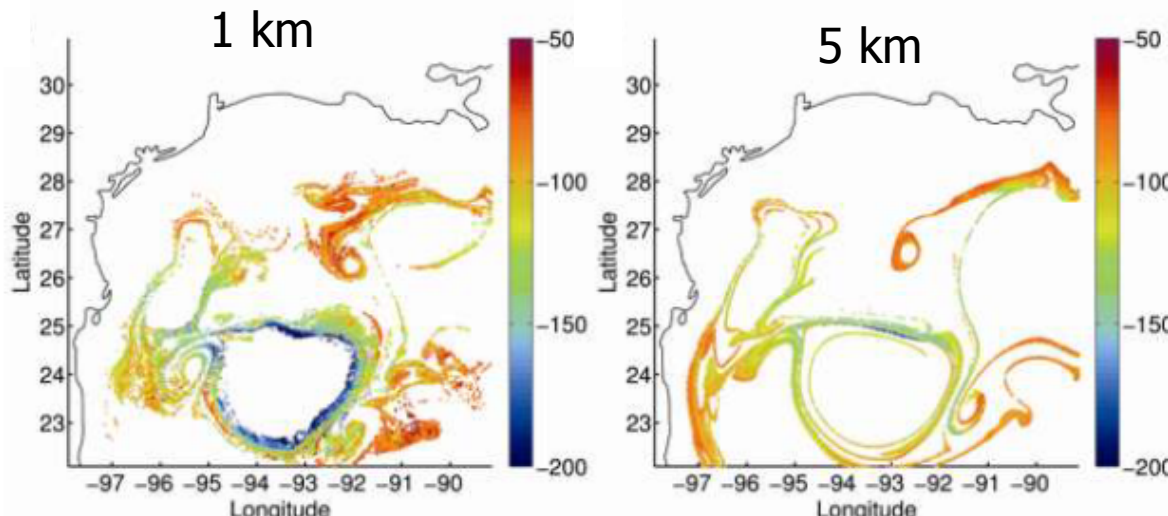
Vertical transects of vertical velocity

w standard deviation  
also shown after  
filtering frequencies  
larger than f

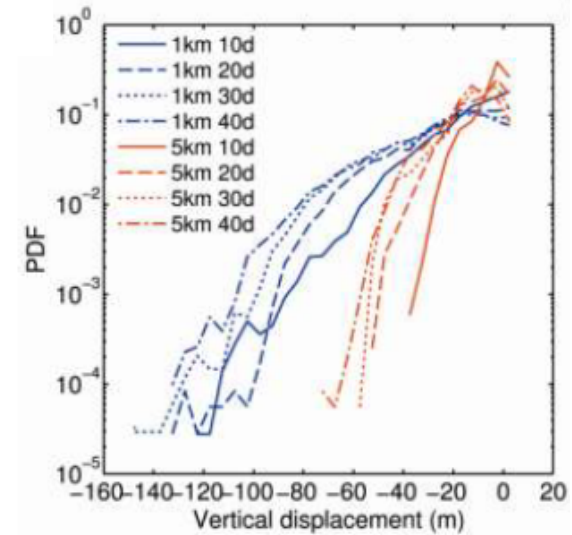
## VERTICAL TRANSPORT: Displacement

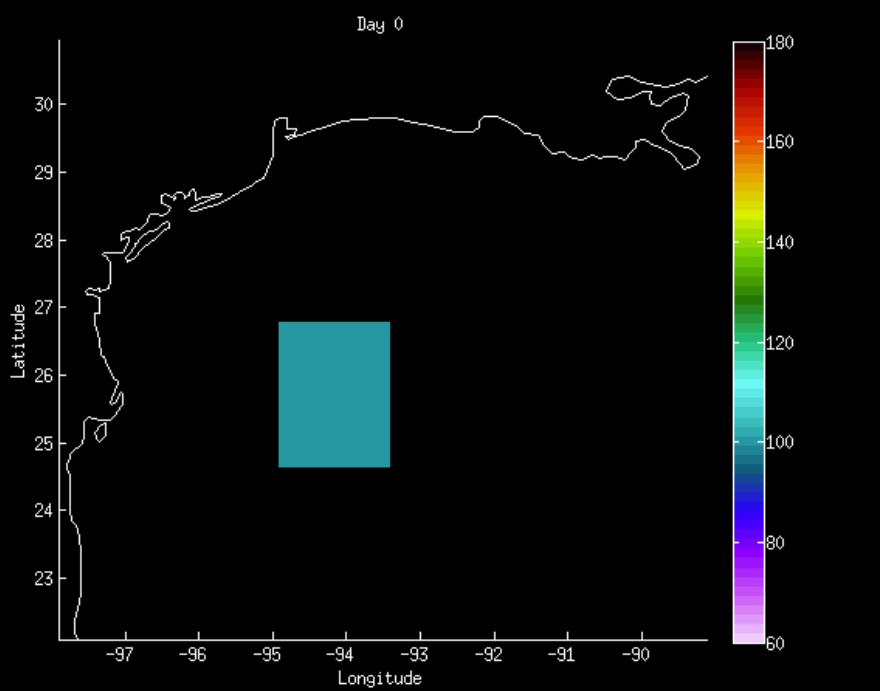
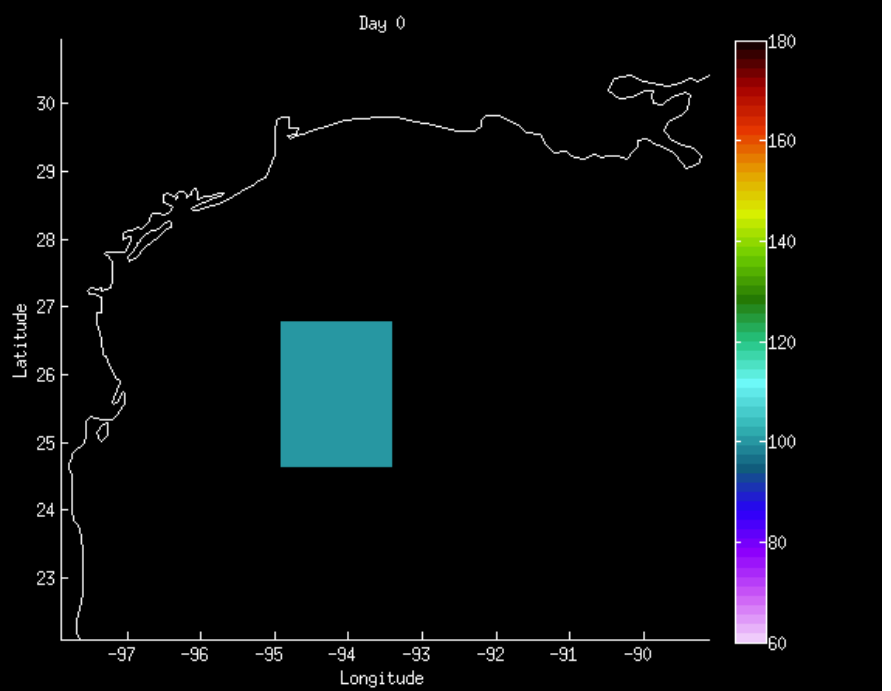
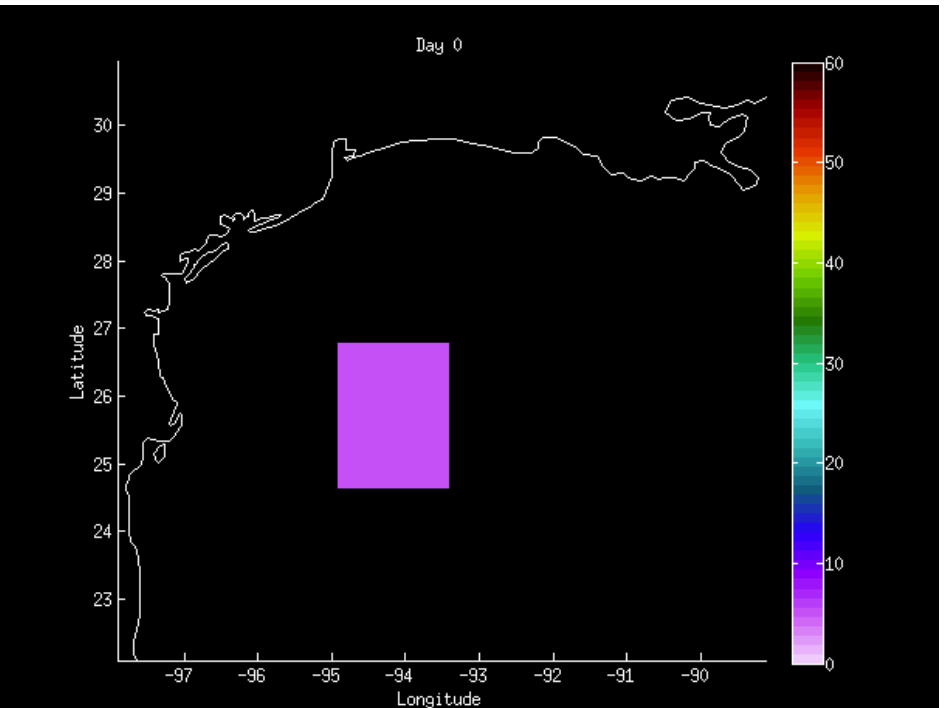
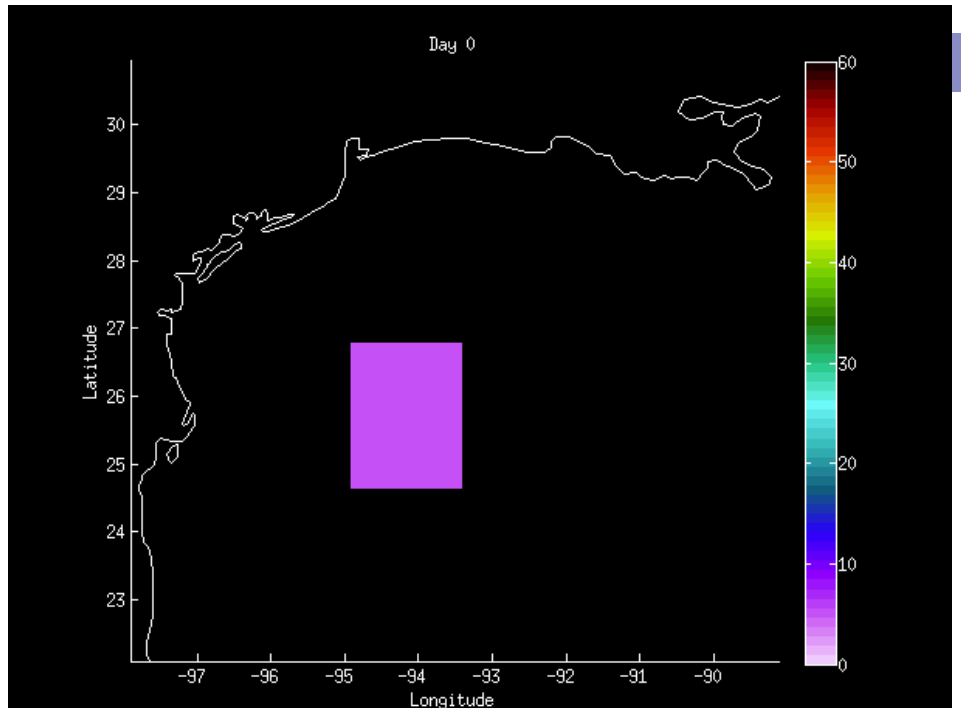


Vertical distribution of 3D particles deployed at 5m (top) and 100m (bottom) 40 days after deployment. Color indicates depth

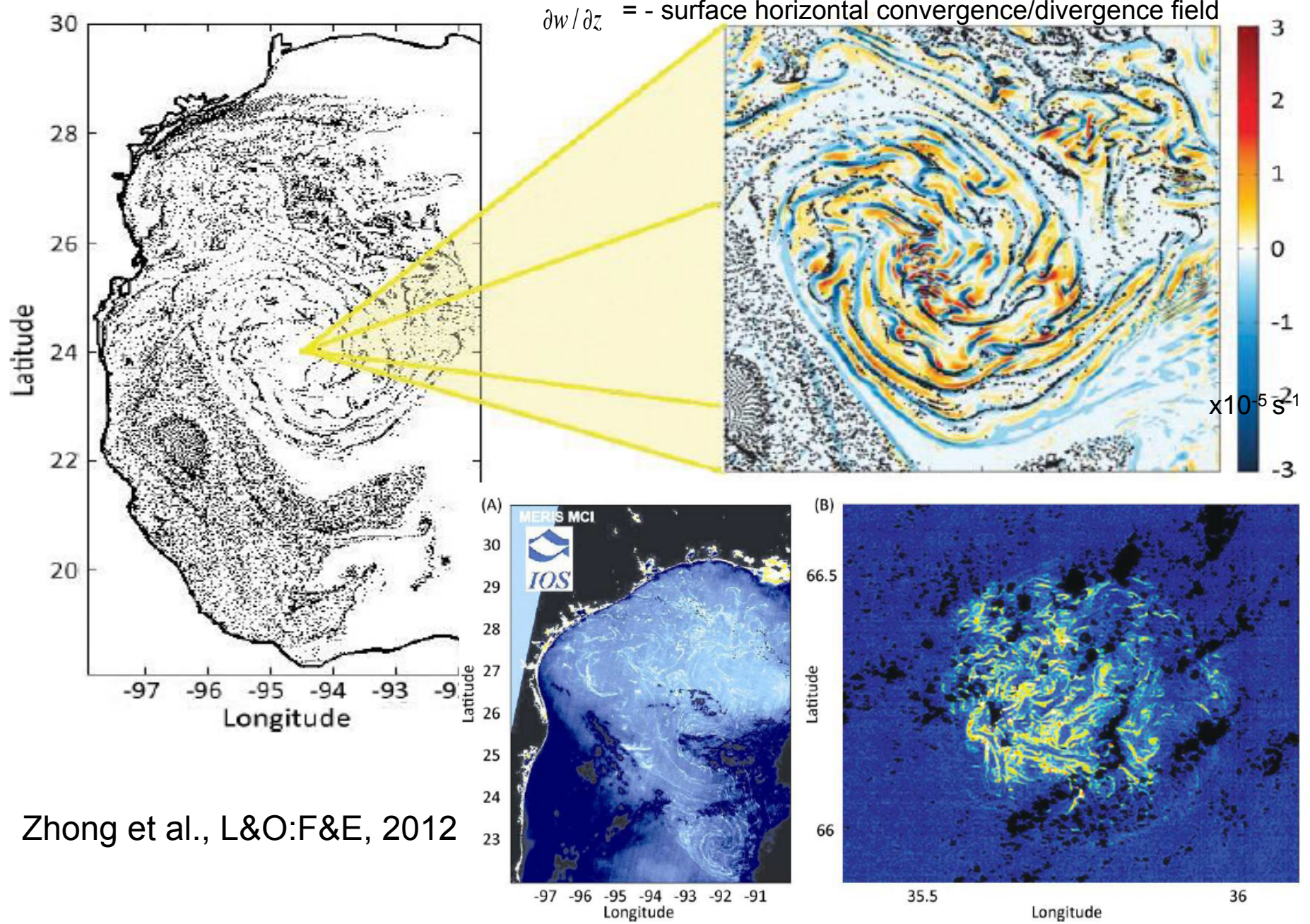


Bottom figure: PDF of displacements for particles deployed at 5m



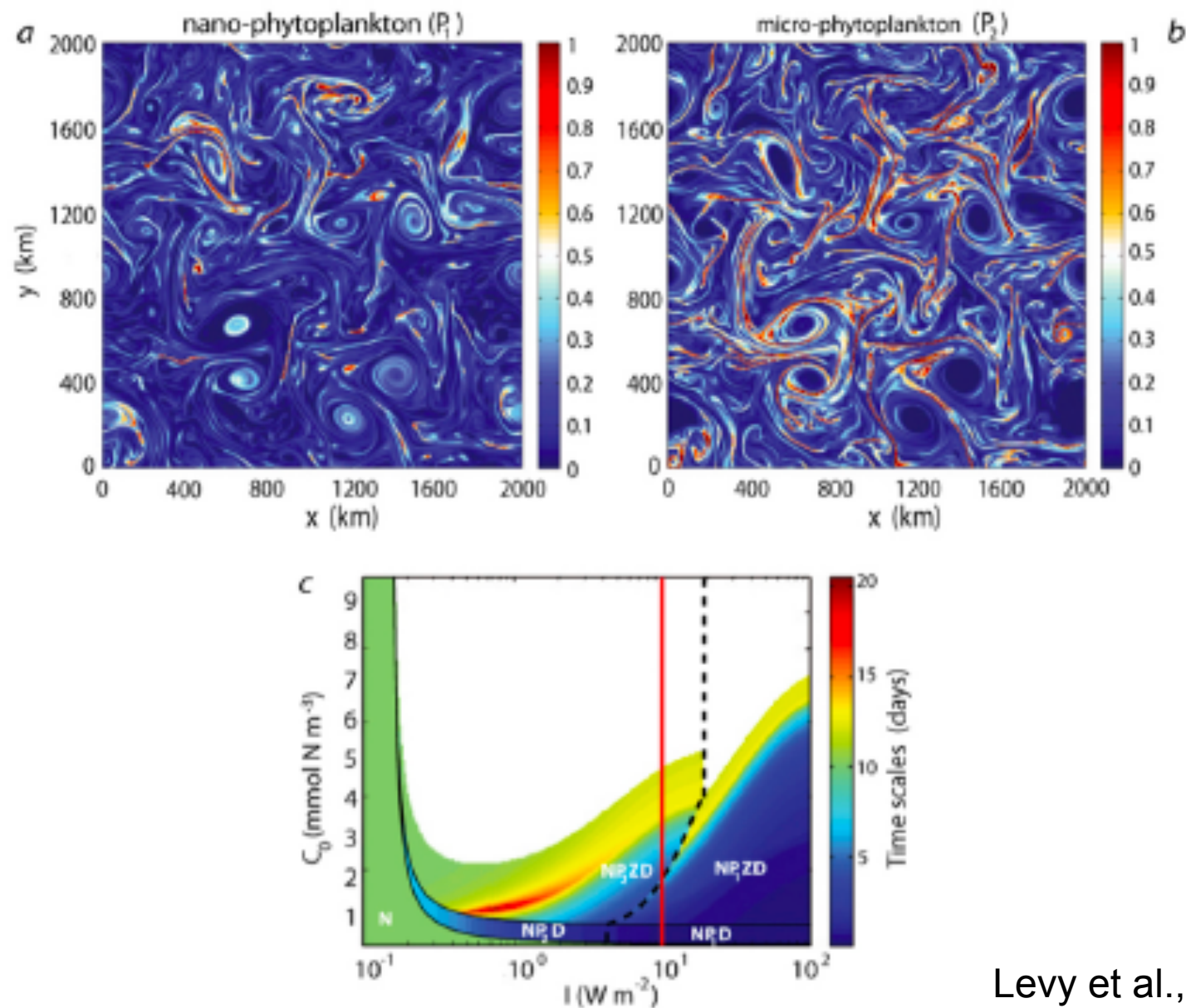


## impact on surface patterns



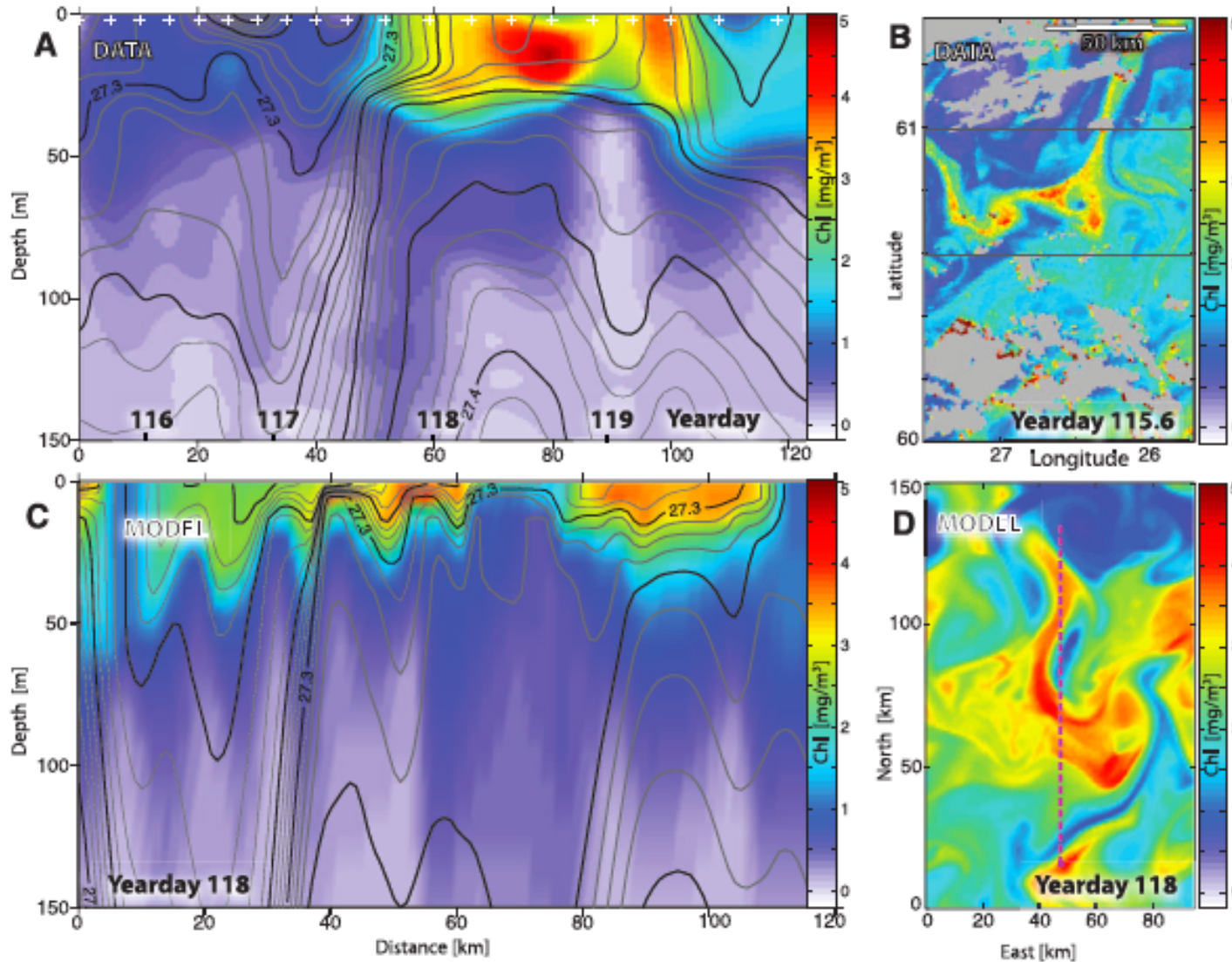
Zhong et al., L&O:F&E, 2012

# impacts on plankton size-classes distributions



Levy et al., GRL 2012

# Impact on bloom initiation



Spring bloom initiation is not due to surface warming but to eddy-driven slumping of N-S density gradients, and it happens 20-30 days earlier than by warming

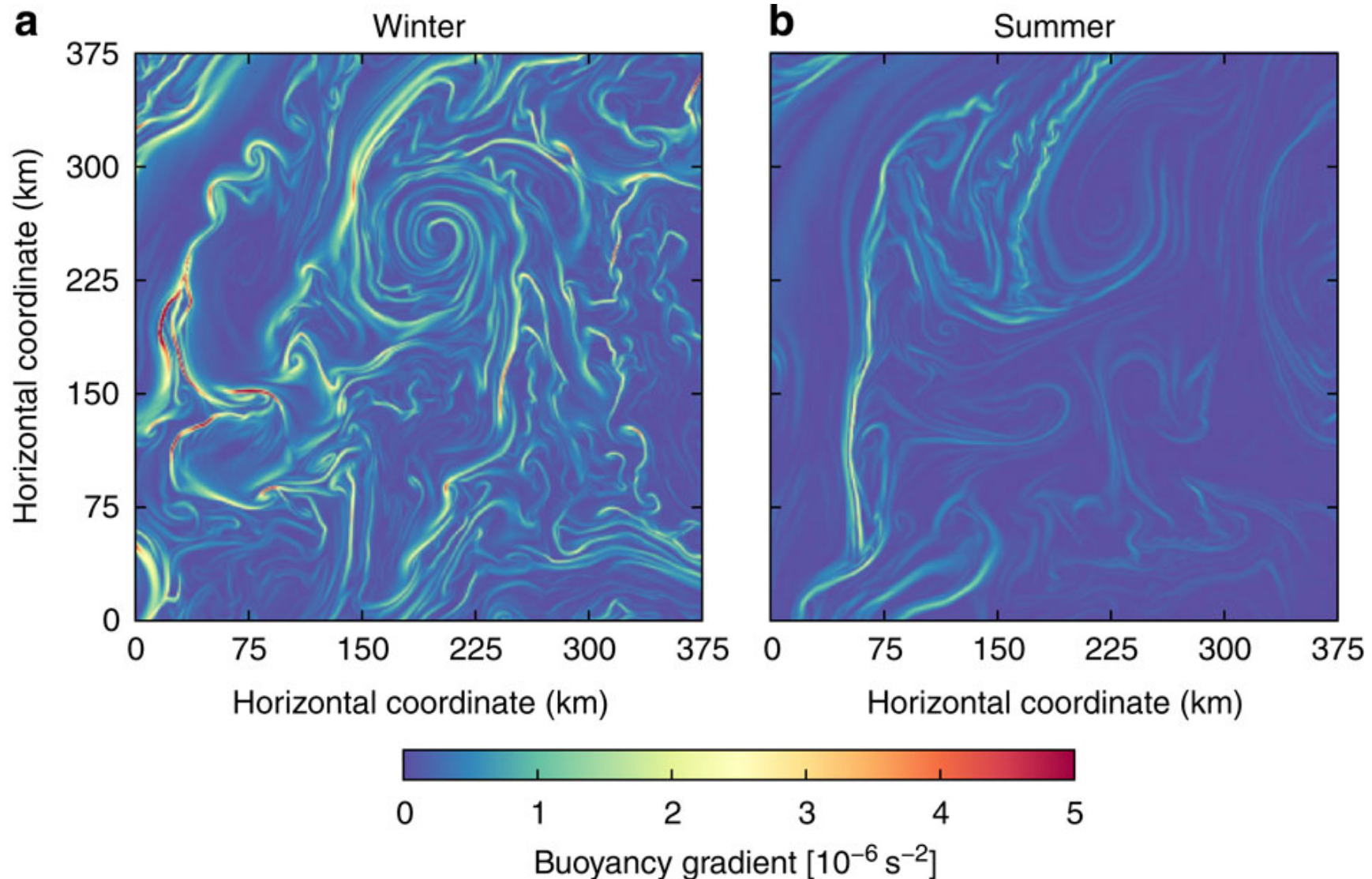
Mahadevan et al.,  
Science, 2012

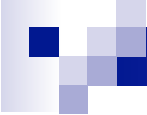


# Seasonality of submesoscale processes

- APE availability depends on mixed layer depth and lateral density gradients. In general, is higher in winter, when the MLD is deeper (Mensa et al., 2013; Callies et al., 2015)
- “However, frontogenetical processes increase horizontal buoyancy gradients when the mixed layer is shallow (i.e. in summer)
- and overturning instabilities weaken the horizontal buoyancy gradients as the mixed layer deepens (i.e. in winter)” Brannigam et al., 2015

# Seasonality of submesoscale processes





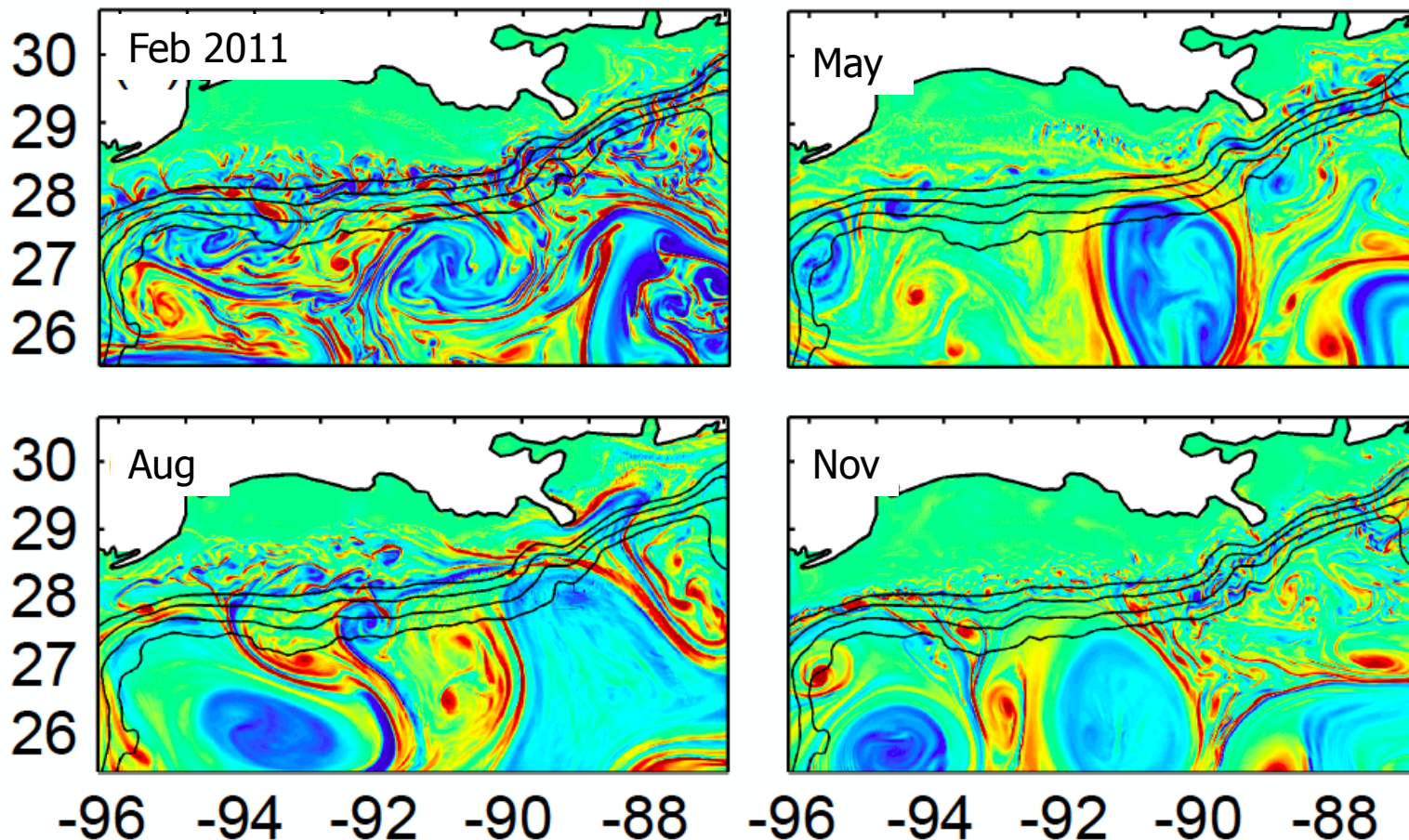
# Is this true everywhere?



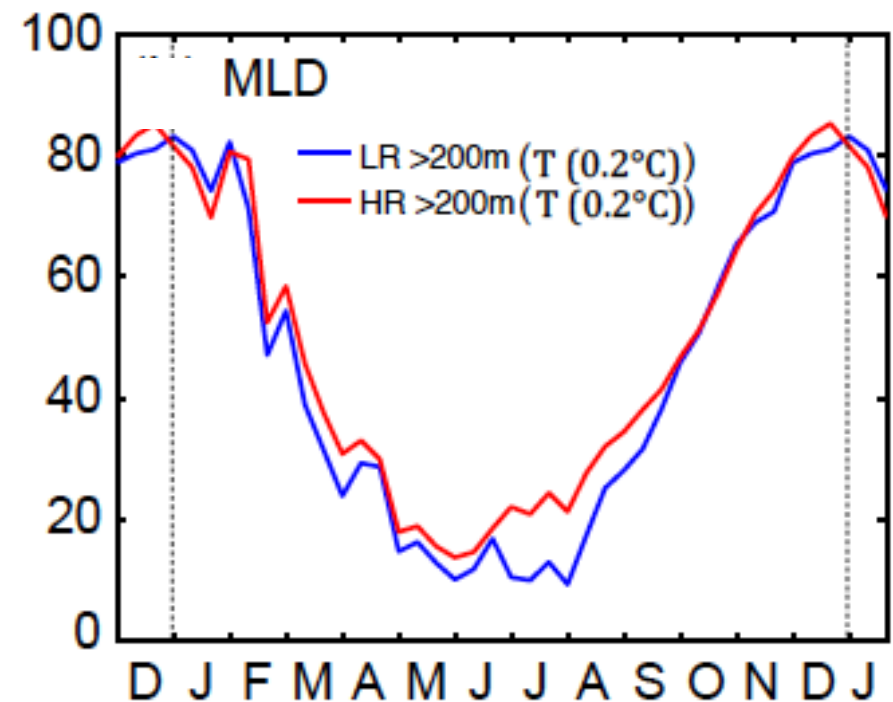
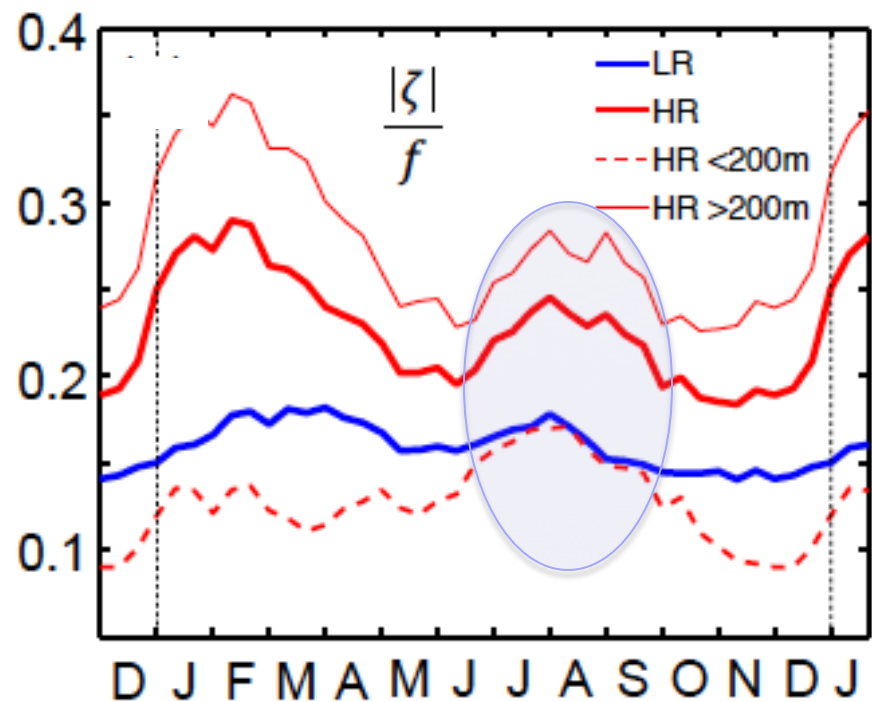


Sea of Marmara Operational Land Imager on the Landsat 8 satellite image of a phytoplankton bloom on May 17, 2015

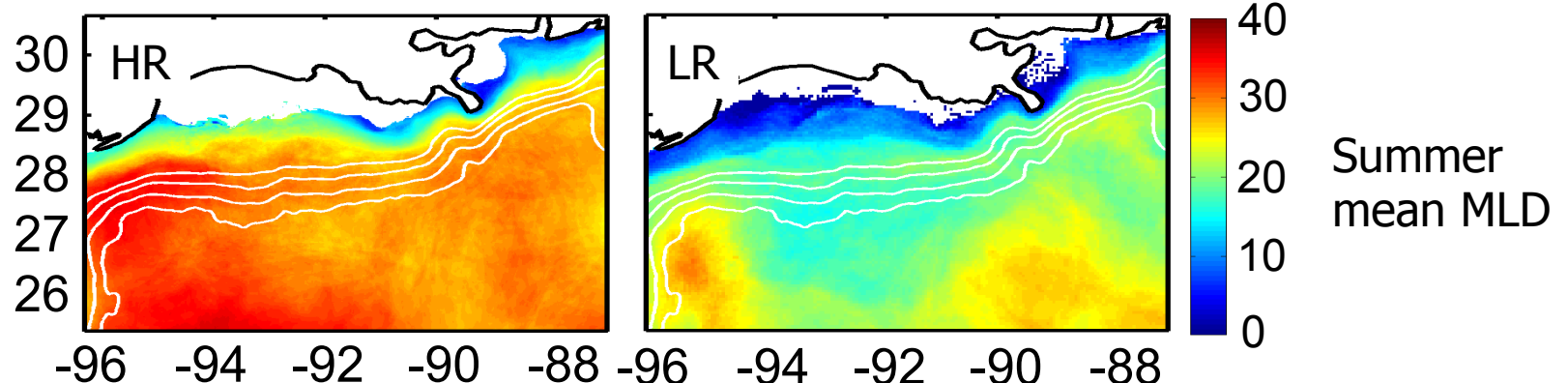
## SEASONALITY OF THE VORTICITY FIELD



- Stronger around the Loop Current and the Rings.
- Enhanced over the slope, weaker on the shelf (especially in winter and fall).
- Wintertime maxima associated with deeper mixed layer

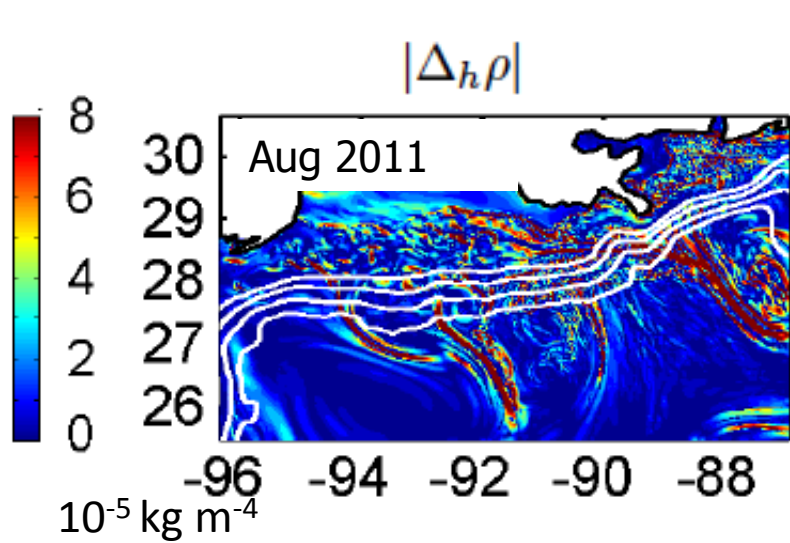
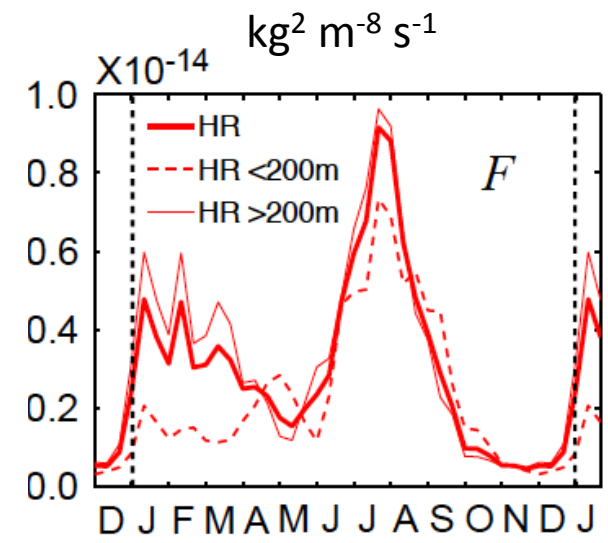
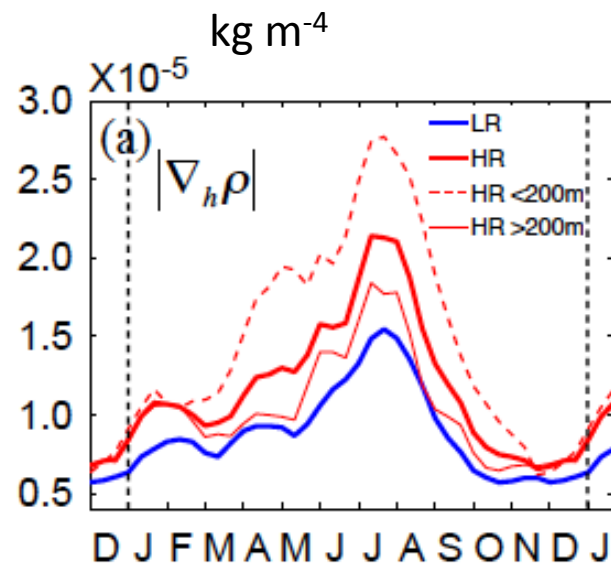
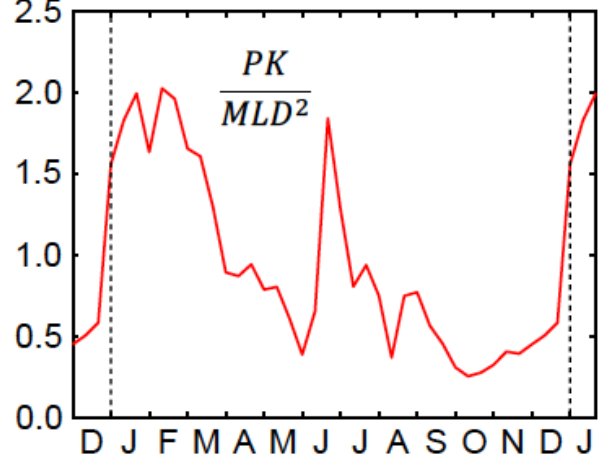


Annual cycle of vorticity and mixed layer depth

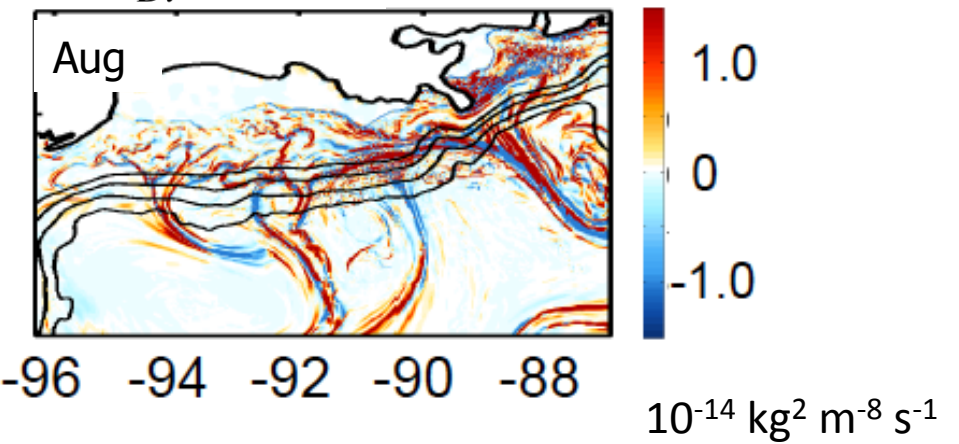


# Other submesoscale variables

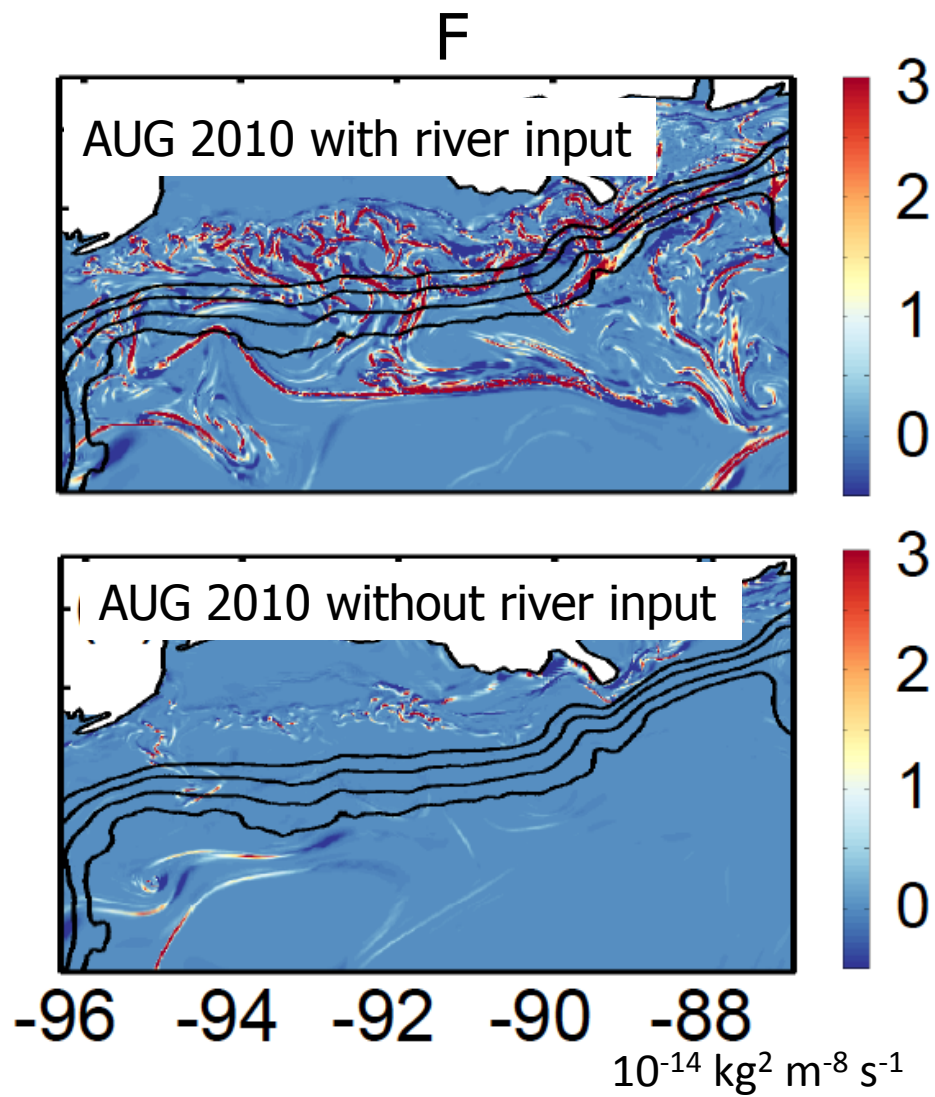
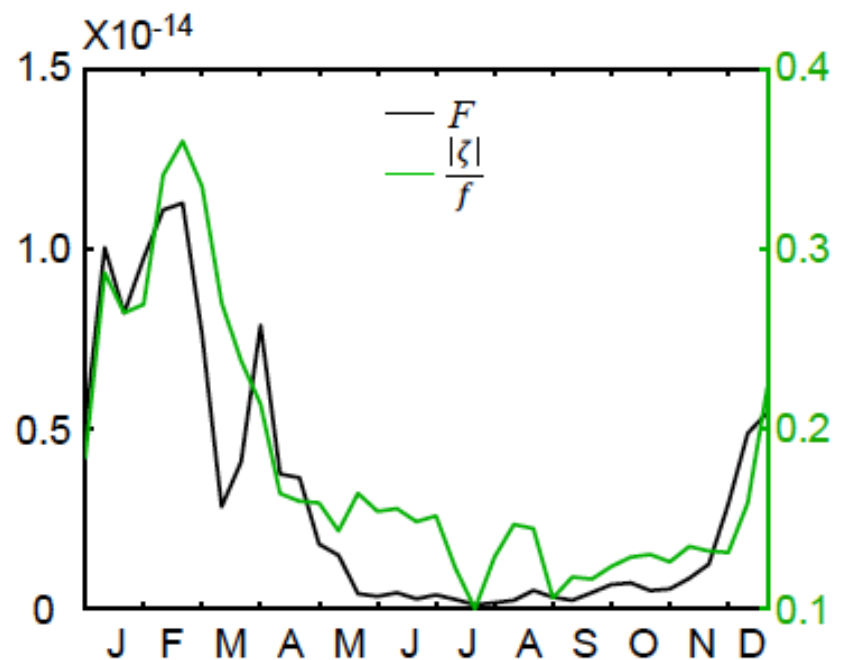
$$m s^{-3} \times 10^{-8} \quad PK = \frac{1}{MLD} \int_0^{-MLD} \langle w'b' \rangle dz$$



$$F = \frac{D |\nabla_h \rho|^2}{Dt} = Q \cdot \nabla_h \rho \quad Q = (Q_1, Q_2) = -\left( \frac{\partial u}{\partial x} \frac{\partial \rho}{\partial x} + \frac{\partial v}{\partial x} \frac{\partial \rho}{\partial y}, \frac{\partial u}{\partial y} \frac{\partial \rho}{\partial x} + \frac{\partial v}{\partial y} \frac{\partial \rho}{\partial y} \right)$$



# In the absence of river input



## Summary and relevance

- Submesoscale expressions (patterns) vary with season and basins. The energy required by submesoscale instabilities to grow is directly proportional to the mixed layer depth but can be supplied through externally driven density anomalies.
- River outflows drive frontogenesis in summer. Given the depth of the mixed layer, summer instabilities are mostly in the shape of elongated fronts
- Any other oceanic regions where river inputs and/or precipitation or ice-freezing and melting are submesoscale hot-spots → Coastal/estuarine areas and of climatic interest the Amazon, Congo, Mekong plume regions, ocean areas affected by monsoonal rain, Antarctica shelves, Greenland shelves, Arctic

# Is this all?

Operational Land Imager on Landsat 8 of large bloom of cyanobacteria in the Baltic Sea

11 August 2015

